

# Lévy walkers inside spherical shells with absorbing boundaries: Towards settling the optimal Lévy walk strategy for random searches

L. G. P. Caramês,<sup>1</sup> Y. B. Matos,<sup>2</sup> F. Bartumeus,<sup>3,4,5</sup> C. G. Bezerra,<sup>1</sup>  
T. Macrì,<sup>1,6</sup> M. G. E. da Luz,<sup>2</sup> E. P. Raposo,<sup>7</sup> and G. M. Viswanathan<sup>1,8</sup>

<sup>1</sup>*Department of Physics, Federal University of Rio Grande do Norte, 59078-900 Natal-RN, Brazil*

<sup>2</sup>*Departamento de Física, Universidade Federal do Paraná, 81531-980 Curitiba-PR, Brazil*

<sup>3</sup>*Centre d'Estudis Avançats de Blanes-CEAB-CSIC, Girona 17300, Spain*

<sup>4</sup>*CREAF, Universitat Autònoma de Barcelona, Cerdanyola del Vallès 08193, Spain*

<sup>5</sup>*ICREA, Institució Catalana de Recerca i Estudis Avançats, Barcelona 08010, Spain*

<sup>6</sup>*ITAMP, Harvard-Smithsonian Center for Astrophysics, Cambridge, Massachusetts 02138, USA*

<sup>7</sup>*Laboratório de Física Teórica e Computacional, Departamento de Física,  
Universidade Federal de Pernambuco, Recife-PE 50670-901, Brazil*

<sup>8</sup>*National Institute of Science and Technology of Complex Systems,  
Federal University of Rio Grande do Norte, 59078-900 Natal, RN, Brazil*

The Lévy flight foraging hypothesis states that organisms must have evolved adaptations to exploit Lévy walk search strategies. Indeed, it is widely accepted that inverse square Lévy walks optimize the search efficiency in foraging with unrestricted revisits (also known as non-destructive foraging). However, a mathematically rigorous demonstration of this for dimensions  $D \geq 2$  is still lacking. Here we study the very closely related problem of a Lévy walker inside annuli or spherical shells with absorbing boundaries. In the limit that corresponds to the foraging with unrestricted revisits, we show that inverse square Lévy walks optimize the search. This constitutes the strongest formal result to date supporting the optimality of inverse square Lévy walks search strategies.

Lévy stable distributions, Lévy walks and flights, have attracted wide attention since the 1990s in areas as diverse as particle kinetics [1, 2] and random lasers [3, 4]. In particular, almost a quarter of a century ago it was proposed [5] that Lévy walks with an inverse square law distribution for the step lengths can lead to optimal search strategies since they maximize the encounter rate with sparse, randomly distributed, revisitable targets when the search restarts in the vicinity of the previously visited target (thus available for further visits) and with no information about the past behavior — an uninformed process. This key fact about “non-destructive foraging” has motivated the formulation of the Lévy flight foraging hypothesis (LFH) in ecology which holds that for many species such optimization may have led to adaptations for Lévy walk search strategies [6, 7]. When originally published, the result caused surprise, because it questioned and then overturned the assumption that organisms move solely according to Brownian motion. In the last couple of decades, however, these results have been exhaustively verified in many different instances [8], becoming widely accepted (see, e.g., Ref. [9]).

More recently there has been renewed interest in certain fundamental and formal aspects of the problem. For example, eventual theoretical findings against the optimality of inverse square Lévy walk searches for any spatial dimensions  $D$  [11] have been shown not to be applicable to the paradigmatic non-destructive random search context [12]. But this debate is understandable given that although several concrete situations have pointed to the aforementioned optimality, it is mathematically very hard to prove (or disprove) and no general developments have appeared so far in the literature.

Aiming to provide an important advance towards finally settling positively the issue, here we study a very closely related problem that is helpfully much easier to deal with. Specifically, we investigate in detail a Lévy walker inside a 2-dimensional annulus with absorbing boundaries. The analysis is also valid for higher dimensions by considering hyperspherical shells. The essential point is that the original foraging problem can thus be analyzed indirectly by proxy, through characterizing the first passage time (FPT) in annuli and shell geometries. Indeed, the first passage time can be thought as the basic building block, representing the finding of successive targets in the random search for many targets, see Fig. 1. The inner boundary represents the previously found target site in the foraging problem. The outer boundary replaces all other targets.

As shown below, our main result is that inverse square Lévy walks strategies become optimal for extremizing the mean FPT when the initial position becomes arbitrarily close to the inner radius. In other words, the first passage time for a Lévy walker to reach the boundary of the annulus or shell is minimized under certain initial conditions that correspond to the case of foraging with unrestricted revisits, i.e., for the non-destructive limit of the original foraging problem.

But before continuing, a few words about commonly used jargon would be in order. The traditional definition of “non-destructive foraging” seems not to capture the most general conditions for the relevant search scenario here. Instead, we adopt the term “foraging with (unrestricted) revisits”. Here by “unrestricted” is meant, e.g., that there is no regenerative (or waiting) times [13, 14] to approach any previously visited target. Nor some targets are more difficult to reach than others,

apart from their Euclidean distance to the walker. Although a subtle difference, we shall make sure that our analysis encompasses a large number of instances, so that the revisits could occur for several reasons besides just retracking regions or areas previously scanned: sensory errors, re-emergent or replenishable targets, heterogeneous target distributions in patches that can be exploited in several visits, and so forth.

The foraging model and the model of search inside annuli and spherical shells are presented in Section I. Sections II and III present analytical and numerical results, respectively. We end with concluding remarks in Section IV.

## I. MODELS

### A. Foraging model:

The foraging model consists of a general strategy rule for the walker (of unit velocity, so that the distance traveled  $L = t$ , with  $t$  the traveled time) to search for targets randomly distributed in a  $D$ -dimensional space (Fig. 1 (a) and (b)):

- (i) If there are targets within a radius of detection (or sight range)  $r_v$ , then the searcher moves in a straight line to the nearest target.
- (ii) If there is no target at distance  $r_v$  from the searcher, then for its  $j$ -th step, the searcher chooses a random direction and draws a distance from a power law tailed probability distribution

$$p(\ell_j) \sim 1/\ell_j^\mu, \quad (1)$$

So, the walker starts moving incrementally, continually looking for a new target within sight radius  $r_v$  along the way. If no target is detected, the searcher stops after covering the distance  $\ell_j$  and (ii) resumes. Otherwise, it proceeds according to rule (i).

The time-averaged search efficiency  $\eta$  is defined as

$$\eta = \lim_{t \rightarrow \infty} N/t, \quad (2)$$

where  $N$  is the number of targets found in time  $t$ .

### B. Search inside annuli and spherical shells

In 1D, the foraging model described above can be solved analytically for the target density going to zero [5, 15, 16]. Specifically, the “mean-field” treatment in Ref. [5] was later rigorously established in Refs. [15, 16] using fractional differential equations with a Riesz kernel. From this framework, one finds that inverse square Lévy walk searches are optimal in the limit of very low target density (ideally vanishing).

In 2D, the problem is substantially more difficult. Numerical simulations have strongly suggested that the

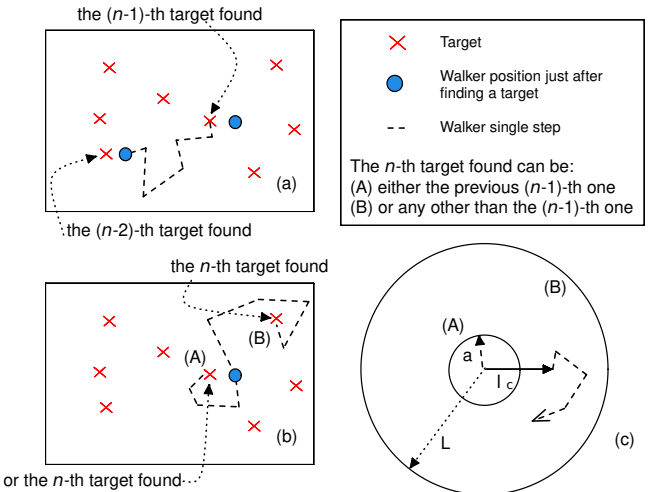


Figure 1. The random search model is depicted in (a)–(b). (a) Always leaving from a position close to the previously found target, the walker follows the Lévy walk strategy (main text) looking for the next target. (b) Once the  $n - 1$ -th target has been found, the  $n$ -th one can be either a revisit to the previous  $n - 1$ -th target — case (A) — or the finding of any other than it — case (B). (c) A random walker (of similar locomotion rules of the random search model) inside an annulus geometry. The circumferences (A) and (B) represent the inner and outer annuli of radii  $a$  and  $L$ .  $l_c$  marks the restart point each time the walker reaches one of the annuli borders. There is a proxy between (A) and (B) in (b) and (A) and (B) in (c), where being absorbing means finding a target.

1D result for the optimality of inverse square Lévy walks extends to 2D and 3D (see, e.g., Ref. [8–10] and references therein). At present, the rigorous analytical treatment of the general 2D problem is considered to be extremely hard, with the eventual exception of the limit that corresponds to the foraging with revisits (which just happens to be the most important case in real applications) as discussed in [12].

*Search inside annuli and spherical shells:* A natural way to tame the original problem, while still retaining most of its important ingredients, is to consider the simpler situation of a Lévy walker inside a 2D annulus, with absorbing boundaries at the inner (border A) and outer (border B) radii, (c) in Fig. 1. Note that to find either the previously found target (the closest one) or any other farther away bears a close relation to reaching either the inner circle border or the outer circle border, Fig. 1. Indeed, the inner circle or sphere represents the previously visited target, whereas the outer circle or sphere represents all the other targets averaged out. Specifically, in passing from the original foraging problem to the annulus problem, the distribution of the distances to the nearest target is replaced by its mean value. Since the distribution has rotational symmetry, the mean distance is independent of the direction. In 2D the locus of points with fixed distance from the previous target is a circle. In  $d$  dimensions it is a  $d - 1$ -dimensional surface

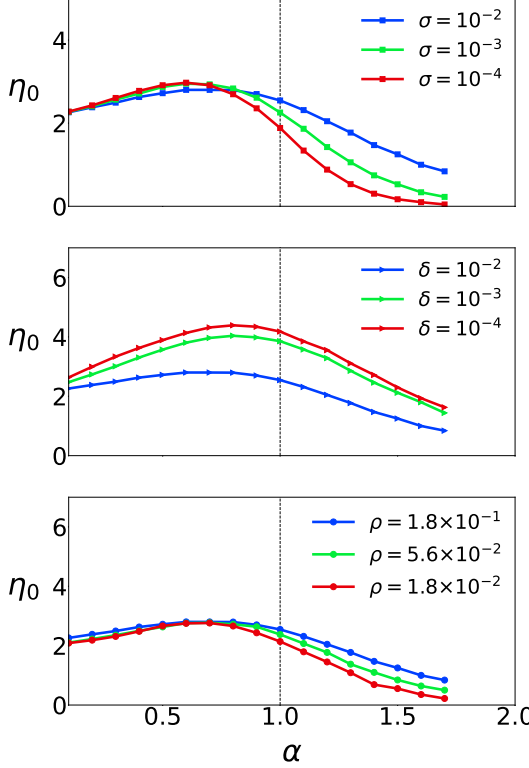


Figure 2. Efficiency  $\eta_0$  as a function of the Lévy index  $\alpha$  for different values of (a) Lévy scale parameter  $\sigma$  ( $\rho = 5.6 \times 10^{-2}$  and  $\delta = 10^{-2}$ ), (b) the relative distance from the inner radius  $\delta$  ( $\sigma = 10^{-2}$  and  $\rho = 5.6 \times 10^{-2}$ ), and (c) the effective density  $\rho$  ( $\sigma, \delta = 10^{-2}$ ). The vertical line  $\alpha = 1$  is just guide for the eye.

of a  $d$ -dimensional sphere.

The dynamics of this simplified model follows the rules:

- (1) The walker always starts (or restarts) at  $(\ell_c, \theta = 0)$ , close to the border of the inner circle ( $\ell_c - a$  is positive but small compared to the outer radius  $L$ ). It then moves between the inner and outer spherical shells, being absorbed upon hitting any of the two.
- (2) At the  $j$ -th step, the walker follows the rule (ii) of the random searcher, with the difference that instead of looking for a target the step terminates if  $\ell_j$  is enough to reach one of the borders, when then (1) resumes.

The FPT efficiency of the above model is characterized as in Eq. (2), but with  $N$  now being the number of times the walker is absorbed by the annuli borders. Very importantly, it is simple to realize that there is a direct correspondence between optimizing the foraging  $\eta$  and minimizing the FPT for the absorbing shells problem.

## II. ANALYTICAL RESULTS

The asymptotic behavior of our random walk inside annuli or  $D$ -dimensional spherical shells of inner radius

$a$  can be obtained analytically in the triple limit

$$l_c \rightarrow a, \quad L \rightarrow \infty, \quad s \rightarrow 0, \quad s < l_c - a. \quad (3)$$

where  $s$  is the scaling factor of the distribution of step lengths. As discussed in [12], this would correspond to the crucial limit of foraging with revisits. The limit  $\delta \rightarrow 0$  means, for the foraging model, that the previously visited target becomes revisitable again almost immediately. In the annulus model, this limit corresponds to being extremely close to the inner circle (remembering that the inner radius corresponds to the radius of detection for the foraging model). The limit  $\sigma \rightarrow 0$  in both models means that the smallest individual random walk steps goes to zero. If this limit is not taken, then when for  $\delta$  sufficiently small, the very first Lévy walk step might be larger than the distance to the previously found target in the foraging model, or else to the inner radius in the annulus model. Specifically, we need  $l_c - a \gg s$  to avoid the problem with the first step being dominant, and this condition is equivalent to  $\delta \gg \sigma$ . Finally, the limit  $\rho \rightarrow 0$  is simply reducing the target density to zero in the foraging model and reducing the equivalent quantity to zero in the annulus model. We have been careful to take the limits in the right order, i.e., first  $\sigma$ , then  $\delta$ , and finally  $\rho$ .

There are many power law tailed distributions, all of which should lead to similar results in this triple limit due to the generalized central limit theorem for Lévy  $\alpha$ -stable distributions [17, 18]. The  $\alpha$ -stable Lévy distribution has the probability density function  $f(x; \alpha, \beta, d, s)$  given by

$$f(x; \alpha, \beta, d, s) = \frac{1}{2\pi} \int_{-\infty}^{\infty} \exp[\phi(t)] \exp[-ixt] dt, \quad (4)$$

with

$$\phi(t) = \begin{cases} itd - |st|^\alpha (1 - i\beta \operatorname{sign}[t] \tan[\frac{\pi}{2}\alpha]), & \text{for } \alpha \neq 1 \\ itd - |st|(1 + i\beta \frac{2}{\pi} \operatorname{sign}[t] \ln[|t|]), & \text{for } \alpha = 1 \end{cases}$$

with  $d, s$  reals and  $\beta \in [-1, 1]$ . The Lévy index  $\alpha \in (0, 2]$  governs the asymptotic behavior of  $f(x; \alpha, \beta, \mu, s)$  in the form of the power-law tail  $\sim 1/x^\mu$ , with  $\mu = \alpha + 1$  for  $\alpha < 2$ . For  $\alpha = 2$  one recovers the Gaussian, since then the second moment is finite and the usual central limit theorem holds. Further,  $\beta$ ,  $d$  and  $s$  represent, respectively, the distribution asymmetry or skewness, shift or location and the scaling for the  $x$  variable.

In what follows, we assume without loss of generality that  $p(\ell)$  is given by  $f(\ell, \alpha, 0, 0, s)$ . Taking  $\beta = d = 0$  is justified because the model should have rotational symmetry (e.g., with  $p(\ell) = p(-\ell)$ ) and then  $s$  can be interpreted as a width. With this choice,  $\mu = \alpha + 1$  for  $\alpha < 2$ .

We also note that there is more than one way of generating Lévy walks in higher dimensions. The method we use here bears resemblance to the uniform model of Lévy walks considered by Zaburdaev *et al.* [19]. Further detailed discussions lie beyond the scope of the present

contribution. Hopefully, this rather technical aspect will be addressed in a future study.

In the foraging problem, there is a well-behaved relationship between the mean free path  $\lambda$  between targets and the target density  $\rho$ . With  $a$  being the radius of detection, in 2D we have  $2a\lambda\rho = 1$ . In  $D$  dimensions, we similarly have  $\rho \sim 1/(a^{D-1}\lambda)$ . Noting that for annuli and shells the mean free path goes with  $L$ , we can define the effective density according to

$$\rho = \frac{1}{a^{D-1}L}. \quad (5)$$

Equation (5) agrees with the definition for the foraging problem up to a constant factor.

Based on Fig. 1 (c) and Eqs. (1) and (2), we can then further define — moreover observing that in fact  $\eta = \eta(\alpha, \delta, \rho, \sigma)$  — that

$$\delta = \frac{l_c}{a} - 1, \quad \sigma = \frac{s}{a}, \quad \eta_0 = \frac{\eta}{\rho a^{D-1}} = \eta L. \quad (6)$$

Note that  $\eta_0$  is adimensional. The important limit  $\delta \rightarrow 0$  (in which the walker is extremely close to the inner annulus of radius  $a$ ) corresponds to the limit of foraging with revisits. Therefore, the curvature of the inner circumference can be neglected: the walker sees the surface of the inner circle or sphere as a “flat wall” regardless the dimension  $D$ . This is the reason why the walker behavior is well approximated by the one-dimensional theory. In this way, the rigorous theory of the Riesz operator [16] on an interval of length  $L$  with absorbing ends becomes applicable [12].

Thence, for  $\sigma > \delta$  the efficiency increases when  $\sigma$  decreases because there are fewer large jumps away from the previous target that makes re-encountering it difficult [12]. When  $\sigma \approx \delta$  the efficiency saturates and should reach its maximum. In fact, for  $\sigma \approx \delta \rightarrow 0$  we must have the same scaling behavior as in  $d = 1$ .

The 1D behavior has been known exactly for a few decades (for details see Refs. [15, 16]). Extending it to the present case, we get

$$\eta_0 \sim \begin{cases} \delta^{-\alpha/2}, & \alpha < 1, \\ \delta^{-1+\alpha/2}, & \alpha > 1. \end{cases} \quad (7)$$

Here it is worth presenting a simplified summary of this optimization result. On the one hand, for  $\alpha > 1$  the mean step size is finite and as  $\alpha$  increases, the searcher spends larger and larger amounts of time backtracking, which increases the time to reach both outer and inner boundaries. The minimum time to reach the boundary is thus given by  $\alpha \leq 1$ . On the other hand, for  $\alpha < 1$  the mean step size diverges and as  $\alpha$  decreases, the probability of reaching the outer boundary on the first step increases, which reduces the probability of reaching the inner boundary which is extremely close. Hence, the optimal efficiency is given by  $\alpha \geq 1$ . The two inequalities,  $\alpha \geq 1$  and  $\alpha \leq 1$ , are of course satisfied only if  $\alpha = 1$ . Eq. (7) is the main result reported here

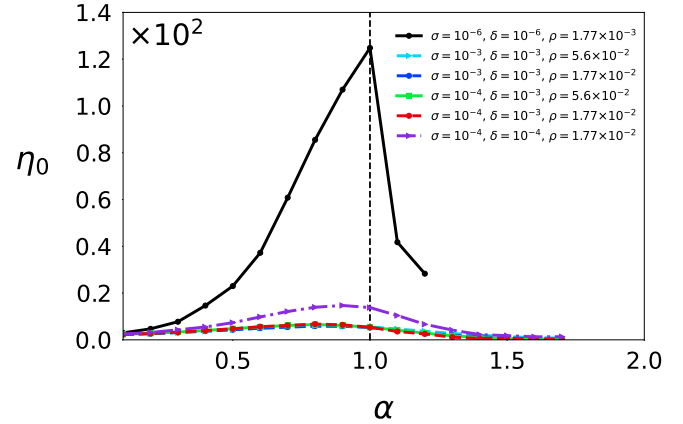


Figure 3. Efficiency  $\eta_0$  as a function of the Lévy index for various values of  $\sigma$ ,  $\delta$ , and  $\rho$  for search inside a 2D annulus. As these parameters tend to zero, the optimal Lévy index goes to 1, corresponding to inverse square Lévy walks. The efficiency  $\eta_0$  is so large for the case  $\sigma = \delta = 10^{-6}$  and  $\rho = 1.77 \times 10^{-3}$  (black curve) that the other curves appear to be zero on a linear scale. For large  $\alpha > 1.2$  some points are not shown because the computational runtime can become extremely large. What is important to note, however, is the behavior near the peak.

for the annulus problem. See appendix B and C for very similar results obtained via alternative arguments, for the foraging problem and the annulus problem respectively.

Thus,  $\eta_0$  has an arbitrarily strong maximum at  $\alpha = 1$  when  $\sigma \approx \delta \rightarrow 0$  in any dimension. This is the key advance reported here.

### III. NUMERICAL RESULTS

In what follows, we verify this theoretical prediction via numerical simulations. Nevertheless, we comment that although a more rigorous and full mathematical treatment of the  $D$ -dimensional is beyond the reach at the present time, still one can derive approximate analytic solutions. We refer the interested reader to the Supplementary Material accompanying the present work (in particular, see Appendices A and B).

*Numerical checks:* Next we present some numerical simulations to corroborate our analytical derivations. First, we consider  $\eta_0$  for small values of pertinent parameters, but not yet fully corresponding to the limit in Eq. (3). In Fig. 2 we plot  $\eta_0$  as a function of  $\alpha$  assuming different  $\sigma$ ,  $\rho$  and  $\delta$ . For instance, when  $\delta$  and  $\rho$  are fixed and  $\sigma$  is decreased, the efficiency  $\eta_0$  for large  $\alpha$  decreased, as seen in Fig. 2 (a). This behavior should be expected since smaller  $\sigma$ ’s implies smaller step sizes, hence making it less probable to reach the target in the first few steps. On the other hand, for  $\sigma$  and  $\delta$  fixed, as  $\rho$  increases the relative prominence of the peak for  $\eta_0$  increases, Fig. 2 (c), again an expected result. Actually, an ever-increasing maximum for  $\eta_0$  is only possible in the

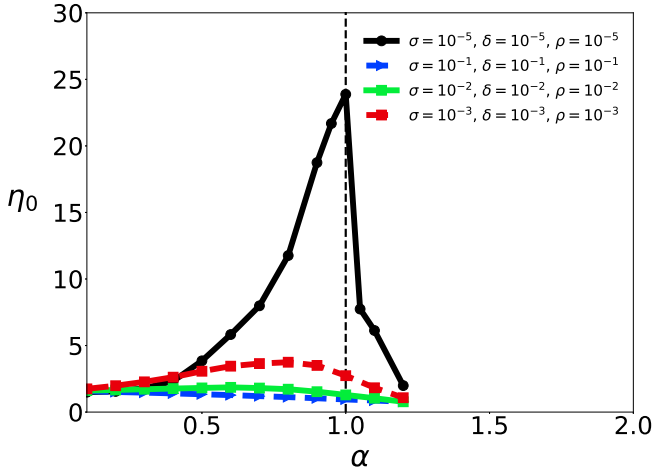


Figure 4. Efficiency  $\eta_0$  as a function of the Lévy index for various values of  $\sigma$ ,  $\delta$  and  $\rho$  for search inside a 3D spherical shell. As predicted theoretically, a maximum emerges near  $\alpha = 1$  as  $\sigma, \delta, \rho \rightarrow 0$ . Again, for  $\alpha > 1.2$  the points are not shown because the computational runtime, even more critical in 3D.

limit  $\rho \rightarrow 0$ . Lastly, by decreasing  $\delta$ , while keeping  $\rho$  and  $\sigma$ , we observe an overall increase of the curve  $\eta_0$  versus  $\alpha$ . This agrees with the fact that for smaller  $\delta$  the searcher will more frequently find the closer target regardless of  $\alpha$ , thus increasing the total efficiency.

If  $\sigma$ ,  $\delta$  and  $\rho$ , Eq. (6), go to zero in a proper manner (see Eq. (3)) we should expect  $\eta_0$  to become arbitrarily large near  $\alpha = 1$ . Exactly as predicted by the theory, Fig. 3 shows how the limit  $\delta, \sigma, \rho \rightarrow 0$  influences the shape of the efficiency curve. Observe that the peak shifts to  $\alpha = 1$  for the case of search with unrestricted revisits. Finally, Fig. 4 shows that likewise the maximum at  $\alpha = 1$  also occurs for search in 3D spherical shells, in precise agreement with our findings.

#### IV. CONCLUSION

We have presented solid analytical results, checked through numerical simulations, showing that the inverse square Lévy walks optimize the time to reach the absorbing boundaries of annuli and spherical shells. Given the relationship of this problem to the original foraging model, these results should be expected to extend to the latter by proxy. Most importantly, our analysis unveils the real reason for the optimality of inverse square Lévy walk search strategies for foraging with unrestricted revisits (hence also non-destructive foraging) in any dimension. Regardless of the dimension  $D$ , the general process essentially reduces to the well-understood 1D model in the case of scarce distribution of targets, not unlike how the approximately spherical earth appears locally flat for small enough organisms. We hope that such findings can finally settle positively

the key fact in the theory of Lévy random search.

#### ACKNOWLEDGMENTS

We thank Sergey V. Buldyrev for very carefully reading our manuscript and giving us very helpful feedback. We thank CAPES, CNPq, and FACEPE for funding. F.B. acknowledges support of Grant CGL2016-78156-C2-1-R from MINECO, Spain.

#### Appendix A: The foraging problem revisited

The foraging problem in 1D is equivalent to a Lévy walker inside an interval with absorbing boundaries. As explained in the main text, the one-dimensional case was rigorously solved in 2001, see Refs. [15,16] (hereafter all cited references refer to those in the main text). In higher dimensions, however, the mathematical difficulties seem to be extremely high, probably demanding the development of new methods and tools for a proper solution. As far as we know, to date the only exception is the triple limit discussed in the main article. However, it is possible to treat the problem approximately, thus obtaining some insight into the main physically important features determining the optimal search strategy. So, in the following we give such an approximate treatment.

In Fig. 5 we show the initial condition of a non-destructive search in 2D. We define the dimensionless parameter  $\delta = (l_c - a)/a$ , with  $l_c$  the searcher initial distance to the nearest target and  $\delta a$  its distance to the circumference of radius  $a$  around the target. We assume the typical length scale  $(\rho a)^{-1}$  calculated for a Lévy walker in 2D, Ref. [11], so that  $\eta = \eta_0 \rho a$ . Comparing with Eq. (5) of Ref. [11], we have that  $\eta_0 = K_d/a$  (the notation  $K_d$  is borrowed from Ref. [11], it represents the efficiency gain). The dimensionless searching efficiency is  $\eta_0(\alpha, \delta, a, s) = f/\langle L \rangle$ , where  $f(\alpha, a, s)$  has dimensions of length (leaving  $\eta_0$  dimensionless) and  $\langle L \rangle(\alpha, \delta, a, s)$  is the average distance traversed until the the encounter of a target. We shall calculate  $\eta_0$  when the search is nondestructive,  $\delta \rightarrow 0$ , and in the scarce regime,  $\rho \rightarrow 0$ .

For  $\delta$  and  $\rho$  going to zero, in 2D the encounter of the very close target (hereafter CT) essentially determines  $\eta_0$ . In fact, in the 2D scarce regime, the probability for the faraway target (FT) — at a typical distance  $\lambda \gg \delta a$  — to be the first one to be found is much lower than  $[\delta a/\lambda]^{\alpha/2}$ , the corresponding probability in 1D. Thus, in 2D with  $\delta \rightarrow 0$  and  $\rho \rightarrow 0$ , to first order one should be concerned essentially with the finding of the CT. Now, to reach this nearby target in the first walk step we need  $\sigma = s/a \approx \delta \rightarrow 0$ , with  $s$  the scale of the  $\alpha$ -stable Lévy distribution (see main text). However, if the searcher eventually misses the CT in the very first step, the next few successive steps still will lead to the CT provided

the searcher does not move away too much from the CT location, say by keeping wandering around within a small region of radius  $na$  for  $n$  few units, see Fig. 5.

Therefore, it is a good approximation to assume that in the above mentioned small region, the fractional diffusion equation that governs the Lévy searcher dynamics leads to solutions displaying basically the same qualitative behavior in 1D and 2D. This way, for  $\delta \rightarrow 0$ ,  $\rho \rightarrow 0$  in 2D we have  $\eta_0 \sim f/(\langle n \rangle_{1D} \langle \ell \rangle)$ , where the 1D result for a Lévy walker starting from a distance  $\delta a \rightarrow 0$  to the absorbing CT within a distance  $na$  can be approximated as in Ref. [5], or

$$\langle n \rangle_{1D} \sim \left( \frac{\delta n a^2}{s^2} \right)^{\alpha/2},$$

and

$$\langle \ell \rangle \sim s \left[ \left( \frac{\delta a}{s} \right)^{1-\alpha} + b \right],$$

where  $b \sim 1$ . We thus get

$$\frac{\langle n \rangle_{1D} \langle \ell \rangle}{f} \sim \frac{a}{f} \delta^{1-\alpha/2}, \text{ with } \delta \rightarrow 0, \rho \rightarrow 0, \alpha > 1$$

and

$$\frac{\langle n \rangle_{1D} \langle \ell \rangle}{f} \sim \frac{a}{f} \left( \frac{a}{s} \right)^{\alpha-1} \delta^{\alpha/2}, \text{ with } \delta \rightarrow 0, \rho \rightarrow 0, \alpha < 1.$$

Then, we obtain in the non-destructive ( $\delta \rightarrow 0$ ) scarce ( $\rho \rightarrow 0$ ) regime that  $\eta_0$  scales with  $\delta$  in the form

$$\eta_0 \sim \begin{cases} \delta^{-1+\alpha/2} & , \alpha > 1, \\ \delta^{-\alpha/2} & , \alpha < 1. \end{cases}$$

We once more shall stress that this is an approximate calculation. A far more grounded procedure is developed in Refs. [15,16]. Nonetheless, the above analysis gives the same result as the more rigorous approach in Ref. [12].

## Appendix B: An approximate analytical treatment for the annulus problem

The 1D equivalent of an annulus or spherical shell is of course just an interval, which has already been discussed in the main text. Moreover, the foraging problem in 1D is identical to the problem of the walker inside an interval (with absorbing boundaries). But although in higher dimensions these two models are not exactly mapped into each other, they are still very closely related.

In the same spirit of the foraging problem in Appendix A, below we present an approximate solution for the absorbing annulus model. It is especially noteworthy that this treatment gives the same answer for the optimality of inverse square Lévy walks in the triple limit  $\sigma, \rho, \delta \rightarrow 0$  obtained in the main text

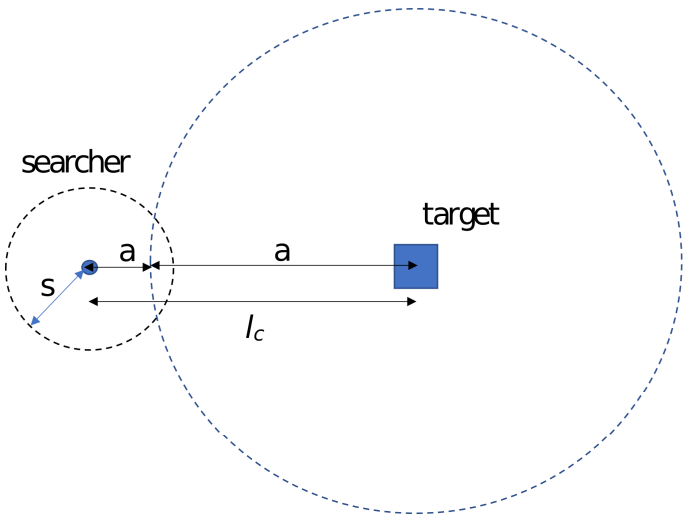


Figure 5. The spatial disposition and relevant distances of the searcher (dot) and nearest target (blue square). The searcher's detection radius is  $a$ , the initial distance from the searcher to the target is  $l_c$ , and  $s$  is the scaling factor of the distribution of step lengths.

through mathematically more well founded arguments. Nonetheless, an interesting aspect of the approach below is that it is a kind of mean field method for the present problem.

The searcher starts from a distance  $l_c$  of the center. For  $\delta = (l_c - a)/a$  as before, we are interested in the  $l_c \rightarrow a \ll b$  limit, i.e.,  $\delta \rightarrow 0^+$  for which the probability of the walker reaching the border  $r = b$  is very small,  $P \ll P_{1D}$ . Note that we can approximate  $P_{1D} = [(l_c - a)/(b - l_c)]^{\alpha/2}$  as the probability of finding the distant site in 1D, with  $P(l)$  power-law with  $\mu = \alpha + 1$  or with a Lévy with index  $\alpha$ . The efficiency can then be written as

$$\eta \approx \frac{1}{\langle n \rangle \langle |l| \rangle}. \quad (B1)$$

Thus, we focus in the case  $\delta \rightarrow 0^+$  for the encounter with the  $r = a$  ring and take into account only the walks that do not stray too far from the  $r = a$  ring. In other words, we restrict the random walk to the region  $r < \gamma a$ , where  $\gamma$  must be of the order of unit. In such framework, the average number of steps is fairly given by the 1D result, but with  $\lambda \rightarrow \gamma a$ . Using  $\eta \simeq 1/[\langle \eta \rangle \langle |l| \rangle]$ , we obtain

$$\eta \sim \begin{cases} \delta^{-\alpha/2}, & \alpha < 1, \\ \delta^{\alpha/2-1}, & \alpha > 1. \end{cases}$$

which coincides with the 2D result in Ref. [12] for the  $\delta \rightarrow 0^+$  limit (assuming a Poissonian distribution of targets

whose density  $\rho \rightarrow 0$ ). That is

$$\langle \eta \rangle_{1D} = f(\alpha) \left[ \frac{x_0(\lambda - x_0)}{s^2} \right]^{\alpha/2} \rightarrow$$

$$\langle \eta \rangle \sim f_{2D}(\alpha) \left[ \frac{\delta a(\gamma a - \delta a)}{s^2} \right]^{\alpha/2}, \quad (B2)$$

where  $s$  is the scale parameter of the Lévy distribution  $P(\ell)$ , defined from its characteristic function  $\bar{P}(k) = e^{-|sk|^\alpha}$  (see also  $\phi(t)$  in the main text).

For a power law instead of a Lévy stable distribution, we can take  $s = l_0$ . The function  $f(\alpha)$  in 1D depends on whether  $P(l)$  is Lévy or power-law, e.g.,  $f(\alpha) = 1/\Gamma(\alpha + 1)$  in the Lévy case (for  $\Gamma$  the Gamma function). But for purposes of scaling laws of  $\langle \eta \rangle$  when  $\delta \rightarrow 0^+$ , this pre-factor is not important once it does not depend on  $\delta$ .

Lastly, to compute  $\langle |l| \rangle$  we also can adapt the calculations for 1D by just supposing walks in the region  $r < \gamma a$ . We can approximate following Ref. [5]

$$\langle |l| \rangle \sim c \left[ \left( \frac{\delta a}{c} \right)^{1-\alpha} g(\eta, \alpha) + h(\alpha) \right]. \quad (B3)$$

Here the functions  $g$  and  $h$  do not depend on  $\delta$ . Thence

$$\langle \eta \rangle \langle |l| \rangle \sim f_{2D} \left[ \frac{\delta a^2(\gamma - \delta)}{c^2} \right]^{\alpha/2} c \left[ \left( \frac{\delta a}{c} \right)^{1-\alpha} g + h \right]. \quad (B4)$$

Taking the limit  $\delta \rightarrow 0^+$

$$\langle \eta \rangle \langle |l| \rangle \sim \begin{cases} \delta^{\alpha/2}, & \alpha < 1, \\ \delta^{-\alpha/2+1}, & \alpha > 1, \end{cases}$$

by retaining only the dependence of  $\langle \eta \rangle \langle |l| \rangle$  on  $\delta$ .

Remarkably, such straightforward and easy-to-understand considerations yields a similar result to the procedure followed in the main text. Recall that in the main text, the steps were as follows: 1. The 2D-search-inside-the annulus problem is first setup. This general problem has not been solved. 2. The limit it taken of  $\sigma \rightarrow 0$ ,  $\delta \rightarrow 0$ ,  $\rho \rightarrow 0$ . In this limit, the problem becomes effectively one dimensional. 3. Eq. (7) is thus obtained in this limit.

But of course, from a fundamental point of view the findings in the main text represent a much more important and rigorous achievement.

### Appendix C: Analytical solution for $\alpha \rightarrow 0$

In the limit where  $\alpha \rightarrow 0$ , the searcher reaches either the outer ring or the inner ring in typically just a single step of size  $\ell$ . We will try to map the step size  $\ell$  into the parameters of concentric rings. For this, we will use the law of cosines:  $L^2 = l_c^2 + \ell^2 - 2l_c\ell \cos(\pi - \theta)$ , with  $\theta$  being the step direction.

If  $L \gg l_c$ , we have that  $\ell = l_c \cos(\pi - \theta) + \sqrt{l_c^2 \cos^2(\pi - \theta) + L^2 - l_c^2}$ , for  $0 \leq \theta < \theta_{\max}$ , where

$$\sin(\pi - \theta_{\max}) = \frac{a}{l_c} \Rightarrow \theta_{\max} = \pi - \arcsin\left(\frac{a}{l_c}\right). \quad (C1)$$

For  $\theta_{\max} \leq \theta \leq \pi$ , we have that  $a^2 = l_c^2 + \ell^2 - 2l_c\ell \cos(\pi - \theta)$ . If  $a < l_c$ ,

$$\ell(\theta) = l_c \cos(\pi - \theta) - \sqrt{l_c^2 \cos^2(\pi - \theta) + a^2 - l_c^2} \quad (C2)$$

. Let  $p(\theta)$  be the PDF of the turning angle  $\theta$ , such that  $\int_0^{2\pi} p(\theta) d\theta = 1$ . This way  $\langle \ell \rangle = \int_0^{2\pi} \ell(\theta) d\theta$ . Substituting in this integral  $\ell(\theta)$  and assuming  $p(\theta) = 1/2\pi$ , it follows that

$$\langle \ell \rangle = \frac{1}{\pi} \int_0^{\theta_{\max}} \sqrt{L^2 - l_c^2 + l_c^2 \cos^2(\pi - \theta)} \, d\theta - \frac{1}{\pi} \int_{\theta_{\max}}^{\pi} \sqrt{a^2 - l_c^2 + l_c^2 \cos^2(\pi - \theta)} \, d\theta, \quad (C3)$$

which leads to

$$\langle \ell \rangle = \frac{1}{\pi} \int_0^{\theta_{\max}} \sqrt{1 - \frac{l_c^2}{L^2} \sin^2 \theta} \, d\theta - \frac{a}{\pi} \int_{\theta_{\max}}^{\pi} \sqrt{1 - \frac{l_c^2}{a^2} \sin^2 \theta} \, d\theta. \quad (C4)$$

Since a second-order elliptical integral function is given by

$$E(\varphi, m) = \int_0^\varphi \sqrt{1 - m \sin^2 \theta} \, d\theta, \quad (C5)$$

then

$$\langle \ell \rangle = \frac{L}{\pi} E\left(\theta_{\max}, \frac{l_c^2}{L^2}\right) + \frac{a}{\pi} E\left(\theta_{\max}, \frac{l_c^2}{a^2}\right) - \frac{a}{\pi} E\left(\pi, \frac{l_c^2}{a^2}\right). \quad (C6)$$

Finally, since

$$\eta = \frac{1}{\langle \ell \rangle}, \quad (C7)$$

we obtain the normalized efficiency as

$$\bar{\eta} = \frac{\eta}{\rho a} = \frac{\eta \pi L^2}{a}, \quad (C8)$$

this efficiency relation, coupled with (C6), allows comparing the efficiency obtained in this section with that obtained in the main text, namely for  $\eta_0$ .

## Appendix D: Renormalization group derivation for the efficiency scaling with $\rho$

As it should be clear from the main text, the association between the foraging and annulus models arises from the fact that the latter represents one target (CT) at the center, the origin, and the mean of all other targets (the FTs) are at the outer radius  $b$ , so that  $\lambda = b$ . Rigorously one should have  $\lambda = b - a$ , but we can neglect  $a$  in the low-density limit since then  $b \gg a$ .

Consider now an annulus with outer radius  $L_0 = 1$  and inner radius  $a$ . In 2D we will define the effective density as usual, according to

$$\rho = 1/(2a\lambda), \quad (D1)$$

where  $\lambda$  is the mean free path  $\lambda = b$ . Further, let  $T$  denote the mean first passage time and  $v = 1$  the adimensional unity velocity, so that

$$\eta = \frac{1}{T}. \quad (D2)$$

If now we have an absorbing annulus system of outer radius  $L \gg L_0$ , obviously its  $\rho$  will be much smaller than the density corresponding to  $L_0$ . We then can use renormalization to map the two cases as the following. We set  $\phi = L/L_0$  and suppose the mapping

$$L \mapsto L/\phi = L_0 = 1 \quad (D3)$$

$$\lambda \mapsto \lambda/\phi = L_0 = 1 \quad (D4)$$

$$a \mapsto a/\phi \quad (D5)$$

$$\rho \mapsto \rho\phi^d \quad (D6)$$

$$s \mapsto s/\phi \quad (D7)$$

$$l_c \mapsto l_c/\phi \quad (D8)$$

$$\delta \mapsto \delta \quad (D9)$$

$$T \mapsto T/\phi \quad (D10)$$

$$\eta \mapsto \eta\phi. \quad (D11)$$

Now, assume that the problem for  $L_0$  has been solved. By recalling that

$$\eta_0 = \eta L, \quad (D12)$$

we have

$$\eta_0 \mapsto \eta_0 [\phi/\phi] = \eta_0. \quad (D13)$$

Since

$$\eta = \eta_0 \rho a^{d-1} \quad (D14)$$

and given that  $\eta_0$  is an invariant of the renormalization group flow map, we can expect to find  $\eta \sim \rho$  for fixed  $a$  and  $\delta$  (so fixed  $l_c$ ).

The above is a non-rigorous scaling argument for the claim first published in Ref. [11] (and stated as proposition (i) in Ref. [12]), namely, that the efficiency  $\eta$  is linear in the density asymptotically. Note that only Eqs. (D3) and (D11) are needed, the other mappings are shown only for greater clarity.

## Appendix E: Algorithm

```
double rng_levy48(double alpha, double rr){
    double ee, phi;
    double mu=alpha;
    double mu1=mu-1;
    double xmu=1/mu;
    double xmu1=xmu-1;
    phi=(drand48()-0.5)*PI;
    ee=-log(drand48());
    return rr*sin(mu*phi)/pow(cos(phi),xmu)
           *pow(cos(phi*mu1)/ee,xmu1);
}
```

The random variables are generated from the Lévy  $\alpha$ -stable distribution with asymmetry parameter  $\beta = 0$  and zero mean, also the scale is  $s=rr$ . The simulations were performed with a homemade code written in C (the language C has been chosen due to speed). The Lévy distributed random numbers were generated using the C code displayed in the chart.

For the computational simulations, the 2D algorithm checks, at each walk, whether or not the Lévy searcher has intercepted the inner or the outer annuli. Figure 6 depicts the algorithm flowchart. We use as parameterization  $r(t) = r_0 + lt$ , where  $r_0$  is the walker starting position.

The algorithm consists of repeating many iterations of the walker always starting a distance  $l_c$  from the center, and performing successive Lévy walk steps one at a time. For each step, possible intersection points of the trajectory and the inner or outer annuli (or shells) are calculated, by simultaneously solving the equations for the line of the trajectory and the circles or shells, considered as quadratic equations for  $D$ -dimensional conic sections. The full procedure allows accessing intermediate values between the points  $r_0$  and  $r_f = r(t=1)$  from the function  $r(t)$ , associating this parameterization to the equations of each annulus. We derive the  $t$  value necessary for the intersection from

$$t_{\text{inner}} = \frac{1}{2A} \left( -B \pm \sqrt{B^2 - 4A(C - a^2)} \right), \quad (E1)$$

$$t_{\text{outer}} = \frac{1}{2A} \left( -B \pm \sqrt{B^2 - 4A(C - L^2)} \right), \quad (E2)$$

with  $A = 2l^2$ ,  $B = 2(x+y)l$  and  $C = x^2 + y^2$ . Therefore, we have two solutions for the inner and two for the outer annulus. Those with values in the interval  $(0, 1]$  indicate that there were one or more intersections. We choose the lowest  $t$  in the interval to compute the distance traveled  $d = lt$ . At the end of the flight, the distance traveled is counted, and there are three possible subsequent actions: (i) if there is an intersection, the searcher will return to the starting point of the simulation,  $(x, y) = (l_c, 0)$ ;

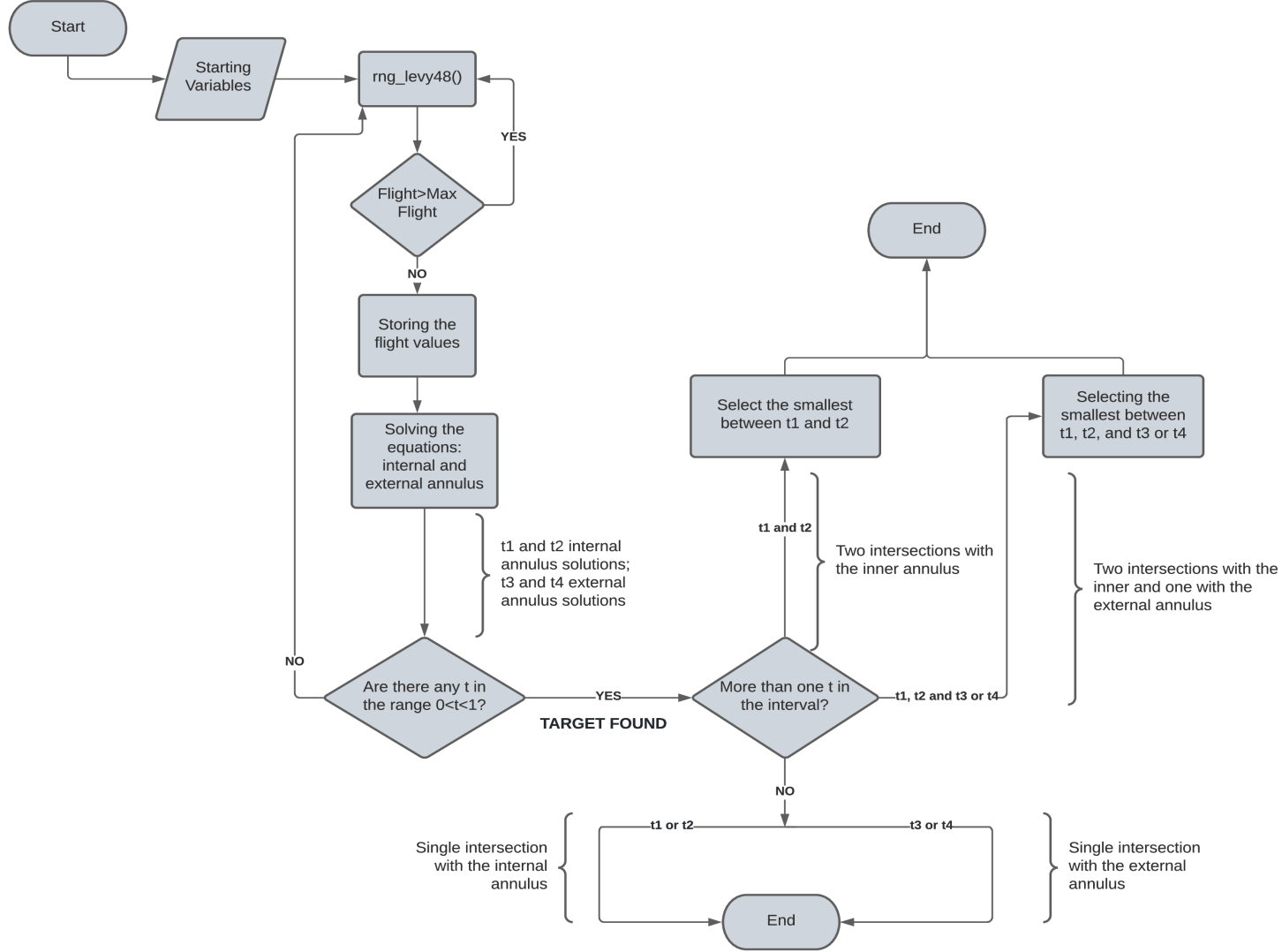


Figure 6. Flowchart of the search algorithm for concentric annuli with absorbing boundaries.

(ii) if there is no intersection, the next flight will depart from  $r_f$ ; (iii) if the total distance value exceeds a certain

threshold, then the simulation ends.

The 3D version of the code was written by adapting the 2D code.

---

[1] V. Zaburdaev, S. Denisov and J. Klafter, Rev. Mod. Phys. **87**, 483 (2015).  
 [2] B. B. Mandelbrot, *The Fractal Geometry of Nature* (Freeman, New York, 1982).  
 [3] A. S. L. Gomes, A. L. Moura, C. B. de Araújo and E. P. Raposo, Prog. Quant. Electron. **78**, 100343 (2021).  
 [4] E. P. Raposo and A. S. L. Gomes, Phys. Rev. A **91**, 043827 (2015).  
 [5] G. M. Viswanathan, S. V. Buldyrev, S. Havlin, M. G. E. da Luz, E. P. Raposo and H. E. Stanley, Nature **401**, 911 (1999).  
 [6] M. G. E. da Luz, E. P. Raposo and G. V. Viswanathan, Phys. Life Rev. **14**, 94 (2015).  
 [7] M. E. Wosniack, M. C. Santos, E. P. Raposo, G. M. Viswanathan and M. G. E. da Luz, Plos Comput. Biol. **13**, e1005774 (2017).  
 [8] F. Bartumeus and S. A. Levin, Proc. Natl. Acad. Sci. U.S.A. **105**, 19072 (2008).  
 [9] G. M. Viswanathan, M. G. E. da Luz, E. P. Raposo and H. E. Stanley, *The Physics of Foraging: An Introduction to Random Searches and Biological Encounters*, 1st ed., (Cambridge University Press, Cambridge, 2011).

- [10] F. Bartumeus, P. Fernández, M. G. E. da Luz, J. Catalan, R. V. Solé and S. A. Levin, Eur. Phys. J. Special Topics **157**(1), 157 (2008).
- [11] N. Levernier, J. Textor, O. Bénichou and R. Voituriez, Phys. Rev. Lett. **124**, 080601 (2020).
- [12] S. V. Buldyrev, E. P. Raposo, F. Bartumeus, S. Havlin, F. R. Rusch, M. G. E. da Luz and G. M. Viswanathan, Phys. Rev. Lett. **126**, 048901 (2021).
- [13] E. P. Raposo, S. V. Buldyrev, M. G. E. da Luz, M. C. Santos, H. E. Stanley and G. M. Viswanathan, Phys. Rev. Lett. **91**, 601 (2003).
- [14] M. C. Santos, E. P. Raposo, G. M. Viswanathan and M. G. E. da LUZ, Europhys. Lett. **67**, 734 (2004).
- [15] S. V. Buldyrev, S. Havlin, A. Ya. Kazakov, M. G. E. da Luz, E. P. Raposo, H. E. Stanley and G. M. Viswanathan, Phys. Rev. E. **64**, 041108 (2001).
- [16] S. V. Buldyrev, M. Gitterman, S. Havlin, A. Ya. Kazakov, M. G. E. da Luz, E. P. Raposo, H. E. Stanley and G. M. Viswanathan, Physica A **302**, 148 (2001).
- [17] B. V. Gnedenko and A. N. Kolmogorov, *Limit Distributions for Sums of Independent Random Variables*, (Addison-Wesley, Cambridge, 1954).
- [18] P. Lévy, *Théorie de l'Addition des Variables Aléatoires*, (Gauthier-Villars, Paris, 1937).
- [19] V. Zaburdaev, I. Fouixon, S. Denisov and E. Barkai, Phys. Rev. Lett. **117**, 270601 (2016).
- [20] A. M. Reynolds and F. Bartumeus, J. Theor. Biol. **260**, 98 (2009).